DOI: 10.17277/amt.2016.01.pp.029-041

The Nature and Multiscale Techniques for Characterizatoin of Mechanical Properties: from Nanostructured Materials to Single Macromolecules

Part I. Theoretical strength. Size effects

Yu.I. Golovin

Institute for Nanotechnologies and Nanomaterials,
G.R. Derzhavin Tambov State University,
33, Internatsionalnaya St., Tambov, 392000, Russian Federation

Tel.: + 7 (4752) 53 26 80. *E-mail:* golovin@tsu.tmb.ru

Abstract

The regularities of changes in the mechanical properties of solids and nanostructured materials with reducing the characteristic sizes of an object, its morphological or structural units up to single molecules are described. Methods of their experimental determination and research are also considered. Particular attention is given to the nature of size effects and atomic mechanism of deformation and fracture in nanoscale. The ways of achieving theoretical ultimate strength and creating high-strength materials are discussed.

Keywords

Mechanical properties of nanostructured materials; nanoindentation; single molecule force spectroscopy; theoretical strength; size effects in mechanical properties; atomic mechanisms of plastic deformation in nanoscale.

Introduction

Mechanical properties are important for three major classes of materials: constructional, structural and functional. For the first two classes they are critical, and for the latter – they largely affect durability and reliability of products, and often their functional characteristics. Since many components of micro- and nanoelectromechanical systems (**MEMS/ NEMS**), data recording and storage devices, sensors, actuators have been reduced up to a submicron size, the mechanical properties of the materials used in them have become essential, especially, in nanoscale. Physical, mechanical, reological and associated properties are also important for biomaterials, which can be regarded either as a kind of functional materials or as a separate class called *soft materials*. Their change affects many functions of biomaterials and objects and can be used as a diagnostic feature. Finally, cross mechano-electrical, electromechanical, magneto-mechanical, mechano-chemical, mechano-emissive and other similar effects and processes are widely used in engineering and to a large extent depend on the mechanical properties of the material.

The most important mechanical properties are considered to be Young's modulus E, shear modulus G, Poisson ratio ν, yield stress σ_y, ultimate strength σ_c and fatigue strength σ_{-1}, coefficients of strain hardening $\alpha = \partial\sigma/\partial\varepsilon$ and rate sensitivity of the flow stress $m = \dfrac{\partial \ln \sigma}{\partial \ln \dot{\varepsilon}}$, viscosity η, hardness H, maximum relative strain up to fracture ε_{max}, fracture toughness K_{1C}. Sometimes some other associated properties are used, such as, fracture energy $A_p = K_{1C}^2\left(1-\nu^2\right)/E$, modulus of plane deformation $E' = E/\left(1-\nu^2\right)$, thermal activation parameters of active plastic deformation, creep and fracture (activation energy U, activation volume γ), tribological, acoustic and other characteristics.

For constructional materials the allowable stresses σ_m are set based on values σ_y or σ_c of the chosen material and accepted assurance factor k_S: $\sigma_m = \sigma_y/k_S$ or $\sigma_m = \sigma_c/k_S$. Then the required section S of the element designed to safely withstand load P (and therefore the weight of construction M) will be

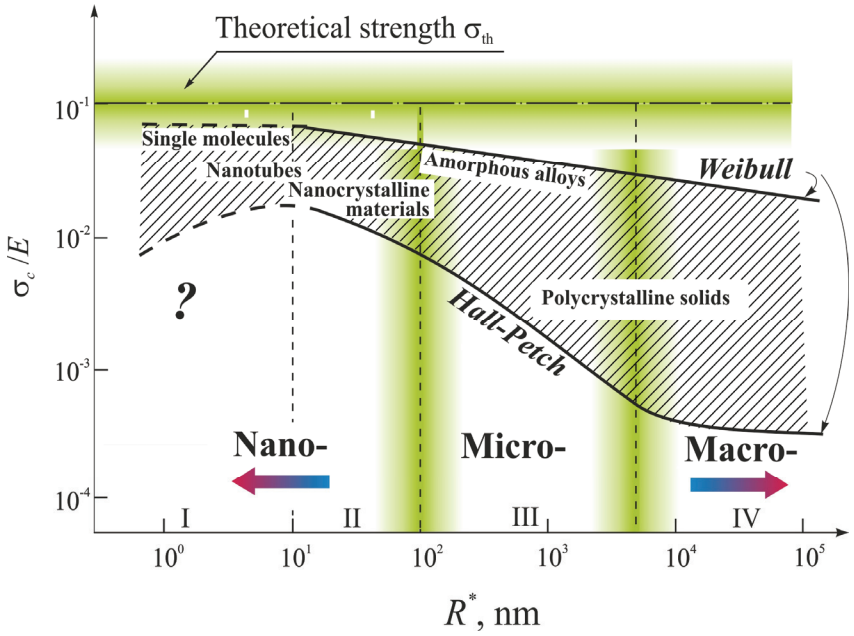

Fig. 1. Schematic diagram of the dependence of mechanical properties of solids on the defining size of the object:
I – a poorly studied region with $R^* \leq 10$ nm; I + II – nanoscale region; III – microscale region of Weibull law effect in polycrystals; IV – region of statistical scale effects, consistent with Weibull theory (for amorphous materials merging with region III)

traumatizing the tissues and easier implanted in a body, etc.

What happens with physico-mechanical and associated properties of materials in a nanoscale region? Experience shows that a decrease in determining size R^* of the object, morphological/structural units of macrobody or a local area of mechanical action from the micrometer to nanometer region, mechanical characteristics can change significantly (often, manifold) [1–3]. With further decrease in R^*, from tens to several nanometers, the course of size dependences of mechanical properties can change dramatically into the reverse one (Fig. 1), where the upper values correspond to the dependences of hardness and ultimate strength on the crosswise sizes of a sample, or the region of the local deformation of single-crystalline materials, while the lower values correspond to the dependence of yield strength on the grain size in a polycrystal. Such behavior in physics is called size effects (**SE**).

inversely proportional to σ_m because $M \sim S \sim (P/\sigma_m)$. Thus, it is the strength that determines the material consumption of static structures, maximum span of bridges and ceilings, ultimate rotations and specific power of piston engines, turbines, machine generators, dynamics, payload and fuel efficiency of vehicles (especially aerospace), the possibility of manufacturing the implants of smaller cross-section and weight, less

The first theoretical estimates made at the beginning of the last century, and subsequent refined calculations showed that in an ideal defect-free crystalline or polymer structure the tensile or shear strength may reach ~ 0.1 of the corresponding elastic modulus E or G (Table 1). This natural ultimate

Table 1

Theoretical strength in different models

Approach	Year	Author	Design formula	Value σ_{th}/E	Value τ_{th}/G
On the basis of the relationship to other mechanical properties	1921	Polyani	$\sigma_{th} = \sqrt{\frac{\gamma E}{d}}$	0,1–0,25	–
	1934	Orovan			
	1926	Frenkel	$\tau_{th} = \frac{G\sigma}{2\pi d}$	–	0,03–0,1
Via estimating the energy of interatomic bonds	1936	de Bur	$\sigma_{th} = n\left(\frac{\partial U}{\partial z}\right)_{\max}$	–	0,08–0,14
Via interatomic potential	1934	Lyav	$U = \frac{A}{r^{12}} - \frac{B}{r^6}$	0,05–0,12	–
	1936	de Bur			
Ab intito from quantum-mechanical calculations	1998	Sob Vitek Li	$\sigma_{th} = A\left(\frac{\partial U}{\partial z}\right)_{\max}$	0,07–0,15	–

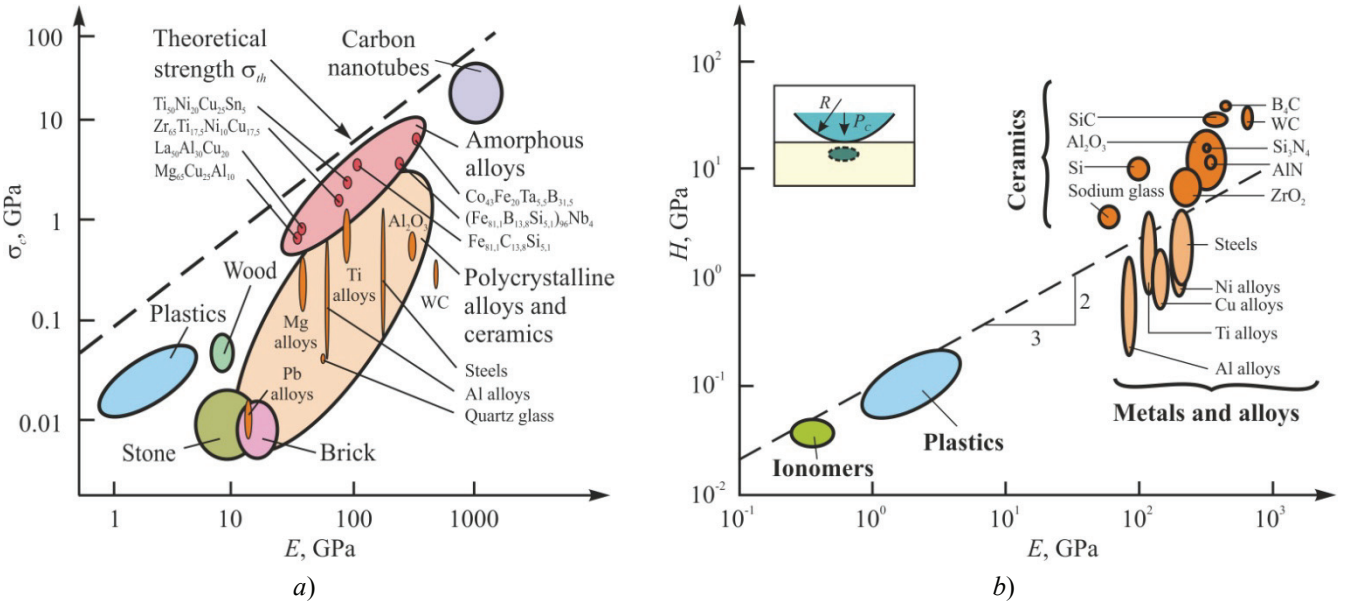

Fig. 2. Schematic diagram of the dependence of critical stresses σ_c of strength (*a*) and hardness (*b*) from the Young modulus (for plastic materials - yield strength, for brittle materials – ultimate bending strength)

strength appears to be a tremendous value, which is difficult to achieve in practice. Only in the early 1970s, Cambridge University scientists [4] managed to approach it while locally loading the annealed gold crystals with a sharpened wire with a radius of curvature at the top of < 100 nm.

According to the authors of [4], plastic deformation in contact started at shear stress $\tau_c \approx 0{,}06\ G$. This value exceeded the macroscopic yield strength of gold dozens of times and was close to the theoretical ultimate shear strength τ_{th}. The beginning of plastic deformation was registered by an electron microscope, in the column of which the experiment was carried out. Practical and theoretical importance of the finding is quite obvious. However, the imperfect methodology at that time did not enable to reliably determine τ_c and identify the regularities of transition from elastic to plastic deformation.

The development of nanomechanical test technology in the last two decades has provided quantitative information about the forces, stresses, deformations and SE in nanoscale. In general, experience shows a direct relationship between strength characteristics and elastic moduli for a wide range of materials (Fig. 2) [5–7]. Unfortunately, an increase in strength of the material is accompanied with a decrease in the ability of materials to withstand the formation and growth of cracks in them (Fig. 3).

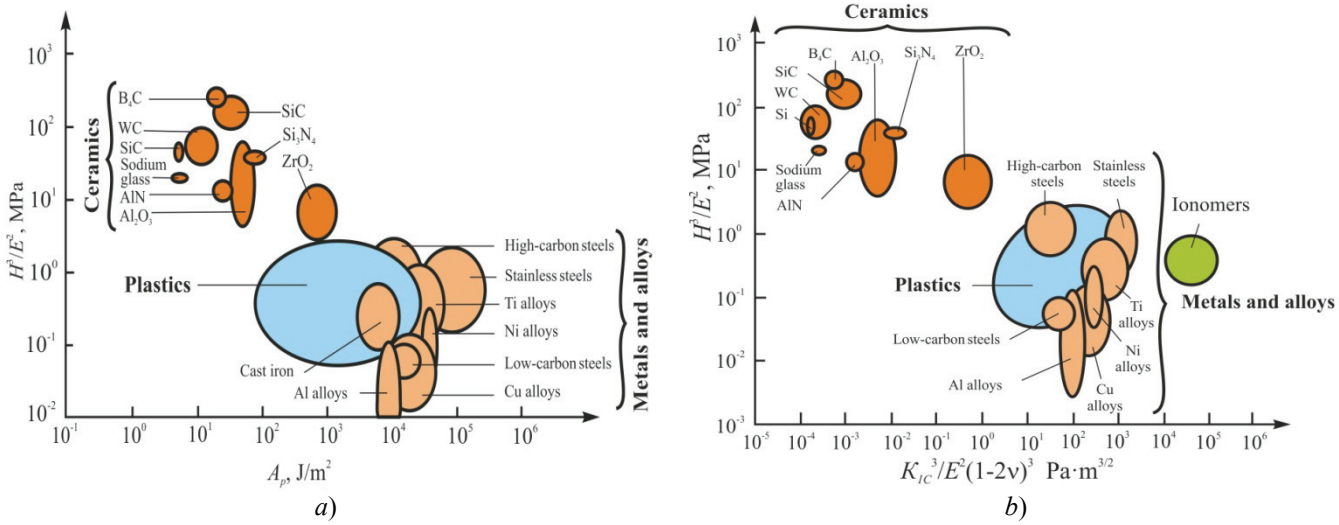

Fig. 3. Relationship between fracture energy G (*a*) and critical stress intensity factor K_{1C} (*b*), hardness H and Young's modulus E

This tendency also retains in nanomaterials, but there are about a dozen of special remedies which can somehow weaken it. [8] Experimental results on the nanomechanical properties of different materials and objects have been repeatedly described in reviews and monographs [1–3, 9–39]. However, the nature of SE in the mechanical properties in nanoscale remains controversial. It is least clear in region $R^* \lesssim 30$–50 nm, where there are SE, abnormal in terms of traditional physics of strength and plasticity.

Mechanics of nanostructures is closely related to their physics and chemistry, because they have single fundamental basis, i.e. specific interatomic interaction. Force, strain, rigidity, viscoelasticity, strength, etc. are of fundamental importance for the biological processes at all structural levels. Any biomechanical process – from unwinding and replication of DNA molecules and intracellular organelle displacement to the cell deformations and displacements – is controlled by molecular forces and nanomechanical properties of single molecules and complexes. In the last decade a significant progress has been achieved in the development of methods for nanomechanical testing and understanding the mechanisms of biomechanical processes at the level of single macromolecules [40]. Since 2008 a specialized magazine "Journal of the Mechanical Behavior of Biomedical Materials" has been published.

The present review focuses on the analysis of experimental and theoretical studies of the last decade, aimed at clarifying the laws and atomic mechanisms of plastic deformation, fracture, friction and wear of materials in nanoscale. As a limiting case there have been considered the results of mechanical spectroscopy of single molecules and their pair interaction. Examples of nanotechnology techniques ensuring the formation of a complex of required properties of the synthesized material due to structural and size factors are given.

The theoretical and real strength of solids

The theoretical, ideal or ultimate tensile strength $\sigma_{th} = F_N/S$ or shear strength $\tau_{th} = F_L/S$ of solids are essentially design values arising from considering the conditions of atomic bonds rupture under the action of applied forces (F_N или F_L), referred to the sample cross-sectional area S (Fig. 4). Several dozens of approaches to the definition of σ_{th} and τ_{th} have been proposed [41–45]. The models under analysis can be classical or quantum-mechanical, numerical or analytical, taking into account or ignoring certain circumstances. Depending on the assumptions made, the design values can slightly vary, accounting for about 0.1 from the corresponding elastic modulus (see. Table 1). Besides, for atomic-scale objects (such as, macromolecules, nanotubes, nanorods) an uncertainty is added due to assumptions about the sizes of atoms and, accordingly, the cross dimensions of the object specifying value S.

The actual strength of even those materials which are considered to be high-strength, in test conditions is below normal values given in Table 1, by 1–2 orders of magnitude. Under such circumstances, some uncertainty in the numerical value of the theoretical strength is not critical for further consideration, and hereinafter, it will be implied by values $\sigma_{th} = 0{,}1E$ and $\tau_{th} = 0{,}1G$.

What causes such a violent discrepancy between theory and experiment? As a rule, while calculating the theoretical strength, a model of perfectly ordered (defect-free) solid in thermodynamic equilibrium is used. However, real materials under normal test conditions or operation are far from equilibrium and contain a number of not only thermodynamic equilibrium defects (their concentration is relatively small), but also excessive, non-equilibrium defects – point, linear (dislocations), two-dimensional (grain, phase, domains boundaries) and three-dimensional (pores, micro-twins, microcracks, etc.) ones. In addition, the condition of the surface and near-surface layers of the sample, temperature, loading rate and duration of the test play an important role. All this taken together can lead to a strong softening of the material. As a result, the real strength of the material is entirely determined by the defect structure, conditions of formation, displacement, interaction and annihilation of structural defects that can be compared to the flow of mechano-induced quasi-chemical reactions in solids. Thus, the mechanical properties of solids are highly structure-dependant that makes us focus primarily on the nomenclature and dynamics of existing or arising under load excessive structural defects.

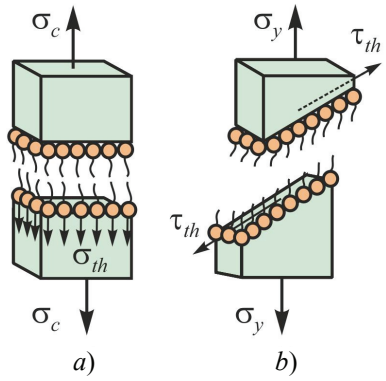

Fig. 4. Diagrams illustrating the definitions of theoretical tensile strength σ_{th} (*a*) and shift strength τ_{th} (*b*)

A shared unsolved problem of plastic deformation theory is that in real conditions a set of elementary flow mechanisms can be implemented simultaneously (concurrently, sequentially or concurrently-sequentially), competing, activating or inhibiting each other. They may be the diffusion (migration) of point defects, dislocation slip and climb, grain turn and slip, twinning, mechano-induced phase transformations with a change in density of the material, and others. As a result, the total rate of relative deformation $\dot{\varepsilon}_{\Sigma}$ is determined by instantaneous sum of the contributions of each *i*-th process

$$\dot{\varepsilon}_i = \partial l_i / l \partial t , \quad (1)$$

where l – a sample size, t – time:

$$\dot{\varepsilon}_{\Sigma} = \sum \dot{\varepsilon}_i . \quad (2)$$

As deformation conditions change (temperature, operating voltage and the speed of their application, the accumulated strain, the characteristic sizes of the loaded region and others), the relationship between $\dot{\varepsilon}_i$ also change that deprives the process of self-similarity, that is, the possibility to be described in a single mechanism. This feature of plastic deformation makes this type of transfer much more complicated than, for example, diffusion, electrical conductivity or thermal conductivity, in which carriers are well-defined (in given cobditions) objects (e.g. atoms, ions, electrons, holes, Cooper pairs, phonons).

Each of the elementary processes of plastic deformation can be considered according to a general scheme typical of kinetic phenomena. As a result, the instantaneous macroscopic velocity of a single process can be represented as the product of the carriers concentration ρ_i, their power b_i and the average ensemble velocity $\langle \upsilon_i \rangle$:

$$\dot{\varepsilon}_i = A_i \rho_i b_i \langle \upsilon_i \rangle , \quad (3)$$

where A_i is a dimensionless coefficient. Depending on the geometric characteristics of the strain and the type of defects that implement it, b_i may have different physical meaning. For example, for glide dislocations b_i is a module of the Burgers vector.

The kinetics of plastic flow can be formally described by the rate constant of quasi-chemical reactions of generation, interaction of the moving strain carriers with scattering and inhibitory centers, annihilation when they meet each other, the surface of the sample, etc. In a very common case the average velocity of glide dislocations is determined by their interaction with a random grid of stoppers. Effective stoppers for glide dislocations are the points of their intersection with dislocations lying in other crystallographic planes, point defects and their few-atomic clusters, grain boundaries, etc. It is easy to show that at ρ = const formally

$$\dot{\varepsilon} = A_g k , \quad (4)$$

where k is a rate constant of bond rupture between a dislocation core and a local stopper; A_g is a constant depending on the geometry of glide.

There are more profound reasons to draw an analogy between plastic flow, fracture and other structural rearrangements, on the one hand, and chemical reactions, on the other hand. Both are controlled by forming, switching and breaking bonds between atoms (molecules), and both, in the vast majority of cases, are thermally activated, as a result of which their macro-kinetics follows the Arrhenius type of equations.

However, the description of micro-mechanisms of plastic deformation and fracture is complicated by a huge number of possible trajectories of the process flow in the configuration space, even if we consider one type of dislocation interacting with one type of local stoppers. If we take into consideration that in a real crystal there exist and interact many different structural defects changing the composition, concentration, and configuration in the process of loading; in dense ensembles of defects there occur strong collective effects, transition of limiting stages and dominant mechanisms in the evolution of the structure, it becomes clear why it is sometimes difficult to establish the true nature of certain mechanical properties by analyzing macro-tests data and predict the mechanical behavior of real materials under load.

Reducing the size of a sample or locally loaded region in addition to increasing the strength of the material makes it possible to approach the elementary acts of plastic deformation and fracture (and sometimes converge their flow to single discrete events) and better understand their nature. If the size reduces significantly, quantum effects and surface phenomena become essential, the importance of mirror image force and line tension for dislocations, the volume and surface diffusion decreases; some deformation carriers are blocked or even no longer emerge, others get benefits. As a result, a complete change in the atomic mechanisms of plastic flow and their limiting steps can occur. This is the central subject under consideration in the description of size effects in physical nanomechanics, and more broadly, taking into account practical tasks – in the formation of new ideas on the ways of creating advanced materials with unique properties.

Size effects in mechanical properties

Size effects occur when one, two or three of the geometric sizes of the object or its internal structure become comparable or less than a characteristic size parameter that determines the state of the structure and kinetics of the process under these conditions (correlation radius, the mean free path, the de Broglie wavelength, critical size of a new phase nucleus, the dislocation loop, micro-twins, etc.). The macroscopic manifestation of SE is a significant change in the thermodynamic and kinetic properties of the material.

In physical nanomechanics the size factor may be:

a) the outer size of the sample;

b) the size across the structural element (agrain in a polycrystal, a phase in a multiphase system, an ordered domain in a polymer), film thickness, or a period of a multilayer heterostructure, etc.);

c) the size of the localized action region (such as the radius of the contact spot under local loading of the sample surface, realized in the process of atomic-force microscopy, nanoindentation, fine grinding in mills, dry friction of micro-rough surfaces, abrasive wear, grinding, etc.) (Fig. 5) [46].

The first observations about the effect of the size of the sample on its structural strength refer to the beginning of the XVI century and belong to Leonardo da Vinci. He found that at equal cross-section that rope is stronger, which is shorter. A century and a half later Edme Mariotte specified: short and long ropes of equal cross-section are able to withstand the same maximum load, but the latter tear more often. In other words, he stated that fracture probability increases with increasing sizes of the products.

In the late thirties of the last century, a probabilistic approach to the description of the strength of materials was generalized by a Swedish engineer

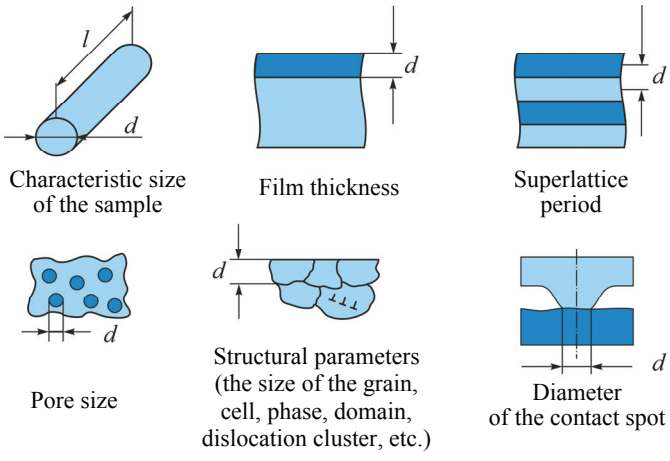

Fig. 5. Some of the most significant factors that dictate size patterns in the mechanical properties of nanomaterials

W. Weibull in the relevant statistical theory, taking into account the increase in the probability P_f of "a weak link" occurrence with the increase in volume V of the sample, which leads to the fracture under stress σ [72]:

$$P_f = 1 - \exp\left[-\frac{V}{V_0}\left(\frac{\sigma - \sigma_0}{\sigma^*}\right)^m\right], \quad (5)$$

where V_0, σ_0 и σ^*, m = 5–50 constants.

According to Weibull theory, size effects in strength are formally derived due to their belonging to basic relations of the sample volume V. It does not specify the physical causes of the observed SE, and also there is no relationship between the size parameters of the theory and linear sizes of the structural elements that really determine the plasticity and strength of material.

Usually statistical theories of strength and plasticity in the spirit of Weibull are used to account for the strength decrease with increasing size of a sample or a product in macro-region, for example, in bridge constructions, dams, etc. They are also useful in the micro- and nanoscale, but their contribution is masked by much stronger structural SE, which is schematically illustrated in Fig. 1.

The first theory of strength taking into account the presence of structural defects, such as, micro-cracks and the effect of stress concentration on them was developed by A. Griffiths at the beginning of the twentieth century. According to it, the strength of the sample (critical stress fracture σ_c) is determined by half-length l of the maximum crack perpendicular to the tensile stress [27]:

$$\sigma_c = \sqrt{2EA_p / \pi l}. \quad (6)$$

In this theory the characteristic size of the problem has a clear physical meaning: it is a crack half-length

In micro-scale ($0{,}1 \lesssim R^* \lesssim 10$ μm) a significant contribution to SE is made by other structural characteristics of the material. In this case as a scaling factor there can be (alongside with the length of the crack and outer sizes of the sample) the characteristic sizes of the internal structure (mean cross-section of the grains in polycrystals or particles of separate phases in alloys, ceramic and composite materials, cells in the dislocation structure; the film thickness or the period of superlattice of multilayer coating on the substrate surface, etc.). To describe SE in this area, the empirical Hall-Petch relationship is widely used:

$$\sigma_y = \sigma_0 + kd^{-n}, \quad (7)$$

where d is the characteristic size of the structure; σ_0, n and k are constants for a given material. In simplest theories $n = 0.5$ that qualitatively (and often quantitatively) agree with the experiment.

Equation (7) is usually a good approximation of the experimental data in the range of $100\ \text{nm} \lesssim d \lesssim 100\ \text{mm}$ and can be justified by simple considerations arising from the dislocation theory of plasticity of crystalline materials [27, 47]. However, in the range of $10\ \text{nm} \lesssim d \lesssim 100\ \text{nm}$, as a rule, there is a considerable deviation from (7), and at $d \lesssim 10$ nm the variation $\sigma_c(d)$ can change into the other opposite one (see Fig. 1). In amorphous solids (in particular, metallic glasses) SE in mechanical properties are generally much weaker than in crystalline materials.

For mechanical testing of microsamples slightly modified traditional means of testing are used; for nanoscale objects several families of special equipment have been developed.

Experimental techniques

For submicro- and nanomechanical testing of consolidated materials and microsamples two large families of devices (Fig. 6) – nanoindenters (for a $10\ \text{nm} \lesssim R^* \lesssim 10$ mm) are used. They implement the principles of instrumented (depth-sensing) nanoindentation (**NI**), and atomic force microscopy (**AFM**) (for $R^* \lesssim 10$ nm) [2]. The latter gives an opportunity not only to obtain the image of the surface with atomic resolution, but also to study its physical and mechanical properties in normal, lateral and mixed contact modes [24].

A set of nodes, their functions and interactions in nanoindenters and atomic force microscopes are similar, besides they have evolved almost in parallel and simultaneously. Resolution of the measurement path of the probe displacement in them is also comparable, and may account for a few hundredths of a nanometer. Nanoindenters use probes with a well defined tip geometry and usually much greater testing force (from micronewtons to several newtons), which together with contact AFM modes allows implementing not only 2D surface research in normal and lateral modes, but also 3D-characterization of mechanical properties to the desired depth (from a few to thousands nanometers). Some of these methods are widely used (for example, those proposed by Oliver and Pharr [48]) and included into international and national standards, particularly into ISO 14577 and ASTM E 2546-07 [49, 50].

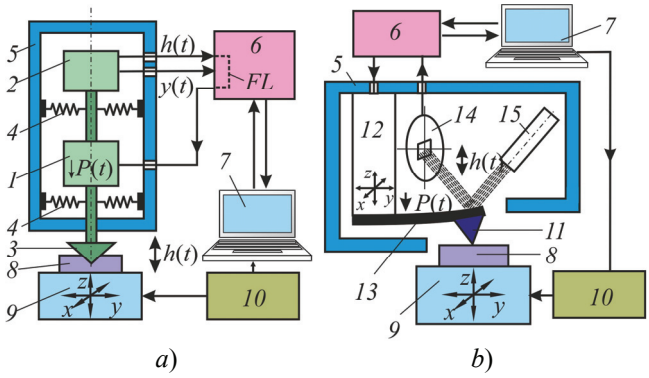

Fig. 6. Schematic diagrams of nanoindenter (*a*) and atomic force microscope (*b*):
1 – power cell; *2* – displacement sensor of indenter rod *3*; *4* – rod suspension springs; *5* – the body of the measuring head; *6* – controller unit; *7* – computer; *8* – sample; *9* – stage; *10* – stage controller; *11* – probe; *12* – piezoelectric actuator; *13* – cantilever; *14* – 4-windows photodiode probe displacement recorder; *15* – laser; *FL* – feedback loop between sensor and actuator

Historically, the first and basic mode of nanoindentometer operation (Fig. 7 *a*) was implemented by indenting geometrically calibrated indenter under the action of a given profile of normal force $P(t)$ and the simultaneous recording of its indentation depth in the material $h(t)$. Sometimes it is useful to present the results in such coordinates, but more often the data is reorganized as dependence $P = f(h)$ (Fig. 7 *b*) which is analogous to diagram $\sigma = f(\varepsilon)$ ("stress – relative deformation") in traditional macrotesting. In some cases, data is presented as dependence of average contact stresses $<\sigma_c>$ от h ($<\sigma_c> = H$ in the area of high P) (Fig. 7 *c*).

In contact micro/nanomechanical tests a variety of loading conditions are used, namely, compression, flexure, tensile, shear, etc. (Fig. 8), as well as probes of different shape, such as, cylinders with a flat end, spheres, cones, pyramids. Each has its advantages and disadvantages. For local testing the most frequently used indenter is a three-sided pyramidal Berkovich indenter. It avoids the problem of bringing the four faces in one point, which is inherent in a widely used Vickers indenter, and when it is necessary to get tip rounding radius of less than 20 nm.

Pyramidal indenter probing leads to the fact that unlike macrotests the deformable sample volume and its characteristic sizes (in particular, h) do not remain unchanged in the process of loading, but increase by many orders of magnitude. The gradients of stress and strain as well as the relative strain rate $\dot{\varepsilon} \sim dh/hdt$ decrease significantly due to the inverse dependence on h. In the absence of SE maximum strain under the indenter remains unchanged under these conditions ($\varepsilon_{max} = 0.1$–0.3, depending on the angle of the tip),

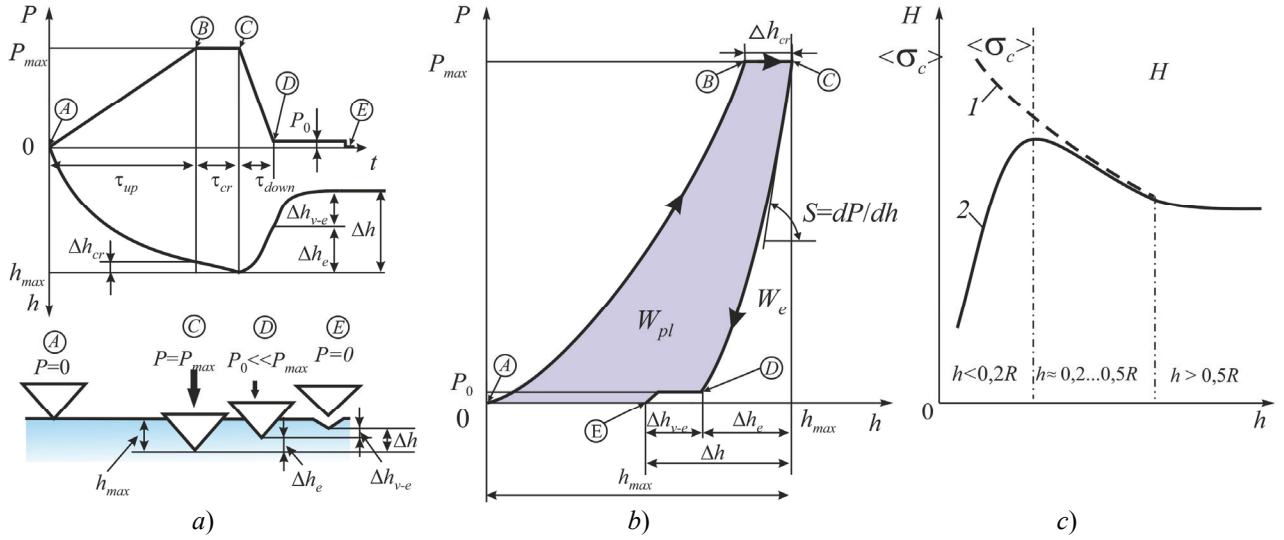

Fig. 7. Three ways of presenting data obtained by normal nanoindentation:
a – in the form of kinetic curves; *b* – in the form of a *P*-*h* diagram (force-deformation); *c* – in the form of Meyer hardness *H* dependence (average contact stress $<\sigma_c>$) on the depth of indentation; 1 – without taking into account the indenter tip blunting; *2* – taking into account spherical blunting. P_{max} – maximum indentation force of the indenter; P_o – a small residual force (~ 3–5 % of P_{max})), required to keep contact with the microhardness indentation in the study of its visco-elastic depth recovery after unloading; τ_{up} – duration of active loading; τ_{cr} – duration of constant loading' τ_{down} – duration of the unloading phase; h_{max} – maximum depth of indentation; Δh_{cr} – increase in the depth of indentation due to the creep; Δh_e – the value of elastic recovery; $\Delta h_{v\text{-}e}$ – the value of visco-elastic recovery (post-effect); Δh – total recovery; W_e – energy of elastic recovery, W_{pl} – energy absorbed and dissipated by the sample in one cycle of loading-unloading; *C* – elastic stiffness of the material in indentation; *R* – rounding radius at the tip of the indenter

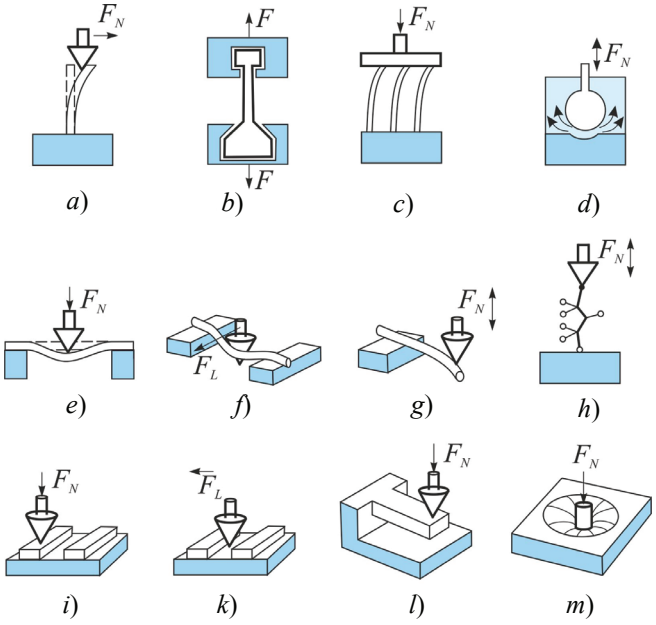

Fig. 8. Schemes of unconventional nano-/ micromechanical tests carried out with NI or AFM:
Cantilever bending tests of quasi-one-dimensional objects (nanotubes, nanofibers, nanowires, nanobelts, etc.) by lateral force F_L (*a*) and stability loss tests according to Euler by normal force F_N (*b* – for single rods; *c* – for a brush of them); tests of visco-elastic surface immersed in a liquid (*g*); three-point bending tests by normal (*d*) and lateral (*e*) force; cantilever bending tests by increasing or oscillating loading (*f*) and uniaxial tensile/ compression tests of macromolecules (*h*); tests of conductive tracks on a substrate by normal indentation (s) and shear stress (*k*); cantilever nanobeam bending tests (*L*) and nanocolumn compression tests (*m*)

and the deformed area spreads on an increasing volume of the material. On the one hand, these features of local loading make it difficult to analyze the results and derive quantitative characteristics of the material and, on the other, in the presence of suitable models and experimental techniques they allow to study size and speed effects during a single loading cycle, scanning the properties along variables h and $\dot{\varepsilon}$. A large number of recently developed methods of processing raw data and their refining from parasitic effects make it possible to derive more than two dozen of different material characteristics and make NI much more informative means of testing than conventional uniaxial tensile/ compression [51–64]. In addition, these techniques allow studying physical and mechanical properties in nanoscale and even at the atomic level that conventional techniques of mechanical tests lack.

Alongside with technical materials, in recent years NI methods have been actively used for testing soft polymeric and biological materials and objects (chitin integument, bone and soft tissues, cells, blood vessels, capillaries, membranes and even single macromolecules) in order to diagnose and early detect various diseases. Most biomaterials are characterized by low stiffness, creep at constant load and visco-elasticity at varying load. In this regard, experimental methods should allow for applying and measuring much smaller forces than in the test of inorganic

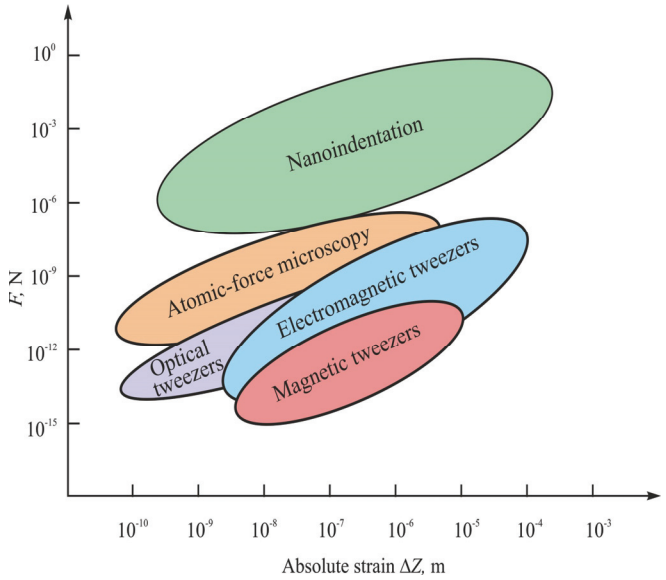

Fig. 9. The operational ranges of forces and absolute strains available for measurements in the five basic techniques of nanomechanical tests

materials, while keeping high spatial resolution and large range of measured deformation.

These needs encouraged, along with further development of NI and AFM methods [65–67], a number of supplementing means: optical, magnetic and electromagnetic tweezers, microneedle manipulators, hydrodynamic stretching of macromolecules along the fluid flow, attaching specific markers (fluorophores, quantum dots) to monitor molecular motion of segments, etc. [40, 68].

Let us dwell on the most popular ones, namely: contact-free tweezers (or otherwise, traps). They allow you to extend the range of applied loads to low forces, however, at the expense of reducing spatial resolution (Fig. 9).

The operating principle of optical tweezers (Fig. 10 *a*) is based on the occurrence of retraction force acting on the dielectric particle placed in inhomogeneous magnetic field. It is created in a laser beam, focused by the high-aperture lens (with aperture NA$\gtrsim$1.2) near one of such particles suspended in a suitable solvent (usually aqueous solution). The interaction of the electromagnetic field of light beam with a dipole moment-induced dielectric particle forces it to retract in the direction opposite to the gradient vector of the electric field in an electromagnetic wave. At small deviations Δr from the equilibrium near the focus ($\Delta r \lesssim 100$ nm) the restoring force is proportional to Δr: $F_e = c\Delta r$. Here c is the rigidity of an optical trap, which has the size orders of magnitude smaller than the softest AFM cantilever. This allows you to apply and measure much smaller test loads (up to hundredths of piconewton).

Plastic or ceramic microspheres, lipid vesicles, cellular organelles and other particles ranging in size from tens of nanometers to several micrometers are used as field-captured particles. They are agents only, taking the force action exerted by the optical trap, which is transmitted to the macromolecule, chemically attached to the surface of the micro-bead. In this way the molecules of DNA, RNA, protein, protein-enzymes, polypeptides, polysaccharides, synthetic polymers and others can be tested. The free end of the tested molecule interacts with a stationary substrate, or any object attached to it, for example, a nanotube, another macromolecule, an antibody, etc. In a different of type optical tweezers a tested molecule is fixed between two dielectric particles captured by two independent laser beams.

The position of a captured particle in space is determined by a non-contact laser interferometer with sub-nanometer resolution. The controlled displacement of the captured molecule ends in one way or another (by moving the beam focus or the substrate stage) leads to a change in the distance Δr between the focus and the center of the captured particle. From these data the values of the acting force and deformation of the tested molecule can be obtained.

Magnetic and electromagnetic tweezers (Fig. 10 *b*) operate in a similar way. In them a dielectric particle is

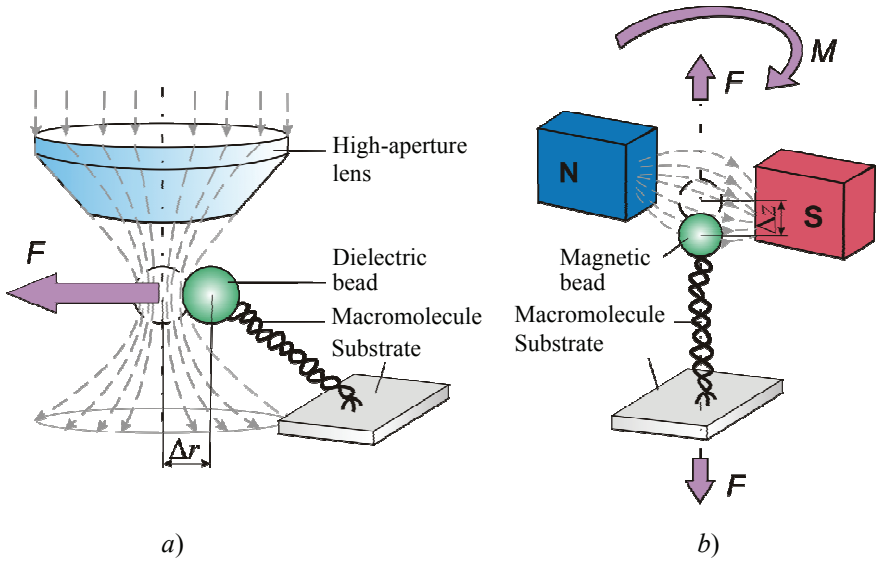

Fig. 10. The scheme of optical (*a*) and magnetic (*b*) tweezers

Table 2

Comparison of the methods of mechanical single-molecule spectroscopy: according to [70] with some corrections and additions

Characteristics	Method		
	Optical tweezers	magnetic/ electromagnetic tweezers	Atomic-force spectroscopy
Spatial resolution, nm	0.1–2	(5–10)/(2–10)	0.1–1
Time resolution, s	10^{-4}	$(10^{-1}–10^{-2})/10^{-4}$	10^{-3}
Rigidity, pN/nm	0.005–1	$(10^{-3}–10^{-6})/10^{-4}$	$10–10^{-5}$
Dynamic range of applied force, pN	0.1–100	$(10^{-3}–10^{-2})/(10^{-4}–10^{4})$	$10–10^{4}$
Dynamic range of measured deformation, nm	$0.1–10^{5}$	$(5–10^{4})/(5–10^{5})$	$0.5–10^{4}$
Probe sizes, μm	0.25–5	0.5–5	Length 100–250 Radius of a tip rounding $10^{-3}–10^{-2}$
Typical applications	3D manipulations, estimation of bonding forces, within intermolecular interaction	The same as those of optical tweezers	Nanomechanical tests and manipulations
Features	Low level of noise and drift. Dumbbell geometry	Force clamp. The possibility of torsion test	The possibility of image of high resolution
Shortages and limitations	Heating and possible damage to a sample by photons. Nonselective capture	Hysteresis in the device	A large probe with relatively high rigidity. High value of minimal applied force

replaced by a ferromagnetic one and drawn into a nonuniform magnetic field generated by permanent magnets or electromagnets, respectively. Retraction force is proportional to the magnetic field induction and its gradient and also displacement Δr of the particle with regard to the magnet poles (at a small value Δr).

To prevent the adhesion of the magnetic particles in suspension they are usually made small enough ($\lesssim 20$ nm) to be in a superparamagnetic state. If it is necessary to obtain a greater force, these superparamagnetic particles are introduced in the inert carrier (often nanoporous), which increases the magnetic moment of the bead. By rotating magnet poles, the torque can be given to a bead. This allows not only tensile but also torsion testing of macromolecules, nanofibers and nanotubes. The approaches described above have a number of varieties and specific means of implementation. Table 2 shows typical characteristics of nanomechanical testing methods outlined above. For more details, you can refer to special and review literature [69–73].

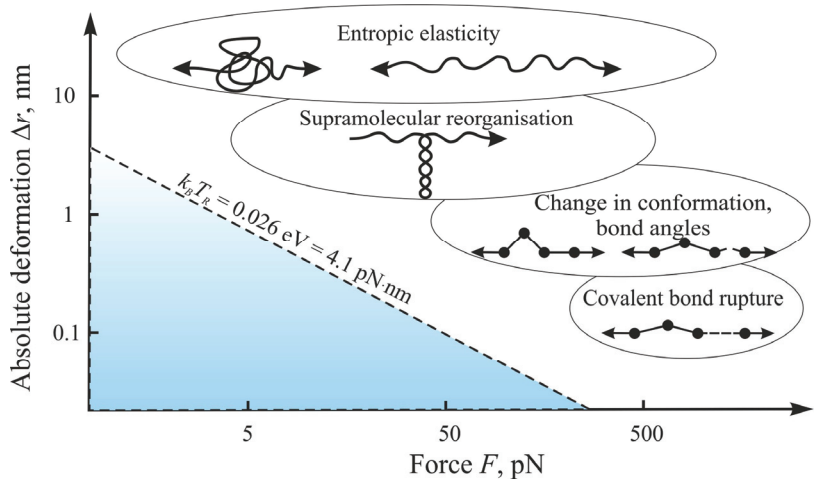

Fig. 11. The range of forces and strains, available for methods of mechanical spectroscopy of single macromolecules. k_BT_R – thermal energy at room temperature [68]

Collectively, optical and magnetic tweezers, allow implementing a large number of nanomechanical studies of macromolecules and their complexes (Fig. 11), comprising determination of critical forces of configuration changes, bond break, changes in chemical and catalytic activity, and others [40, 68, 72].

In recent years, in addition to improving the means of proper nanomechanical tests [74–81], there

appeared combined approaches using the possibilities of other physical methods: in situ electron microscopy [82–86], acoustic [87–89], X-ray and electron microdiffraction [83, 85, 90], micro-Raman spectroscopy [91], electrical [92–95], fluorescence [96] small-angle neutron scattering [97], tomography of atomic resolution [98], and others.

Conclusion

Taken together, experimental methods of nanomechanical and combined tests can solve the following problems:

– engineering characterization of physical and mechanical properties of materials in nanoscale;

– basic research into the nature of these properties, the atomic mechanisms of deformation and fracture and size effects in the mechanical properties;

– replacing single destructive macrotests by repeated non-destructive tests (in size-independent area);

– physical modeling of friction and wear with atomic resolution at the level of a single dynamic nanocontact and single atoms;

– determination of physical and mechanical properties of biomaterials and biological objects (tissues, cells, membranes, capillaries, etc.) to clarify the mechanisms of their functioning, biochemical reactions (at the level of single macromolecules), the dynamics of elementary acts and intermediate states, as well as early diagnosis of diseases.

Acknowledgments

This work was supported by the Russian Science Foundation (RSF) grant № 15-19-00181 Technique and nanoindentation data analysis, size effects on hardness; RSF grant 14-13-0073 Technique and analysis of single-molecule force spectroscopy data; the Ministry of Education and Science of the Russian Federation grant K1-2014-022 (Theory and calculations of mechanical properties and dynamics of macromolecules, analysis of the existing models of theoretical and real strength of materials).

References

1. Gogotsi, Y., ed. (2006). *Nanomaterials Handbook.* CRS Press. Boca Raton, Fl.: Taylor & Francis, 780 p.

2. Bhushan, B., ed. (2010). *Springer Handbook of Nanotechnology.* New York: Springer, 1916 p.

3. Andrievskiy, R.A. and Glezer, A.M. (2009). *Uspehi fiz. Nauk* [Advances in physical sciences], 179, 337. (Rus)

4. Gane, N. and Cox, J.M. (1970). *Phil. Mag*., 22, 881.

5. Ashby, M.F. and Greer, A.L. (2006). *Scripta Mater*., 54, 321.

6. Zok, F.W. and Miserez, A. (2007). *Acta Mater*., 55, 6365.

7. Greer, A.L. (2009)/ *Materials Today*, 12, 14.

8. Ma, E. (2006). *JOM*, 58, 4.

9. Eliseev, A.A. and Lukashin, A.V. (2010). *Funktsionalnyie materialyi* [Functional Materials]. M.: Fizmatlit, 456 p. (Rus)

10. Tretyakov, Yu.D. and Gudilin, E.A. (2009). *Uspehi himii* [Advances in Chemistry], 78, 876. (Rus)

11. Suzdalev, I.P. (2009). *Uspehi himii* [Advances in Chemistry], 78, 266. (Rus)

12. Valiev, R.Z. and Aleksandrov, A.V. (2007). *Ob'emnyie nanostrukturnyie metallyi: poluchenie, struktura i svoystva* [3D nanostructured metals: production, structure and properties]. M.: IKTS, 398 p. (Rus)

13. *Metallopolimernyie nanokompozityi (poluchenie, svoystva, primenenie)* [Metal-polymer nanocomposites: production, properties, application], Novosibirsk: Izd-vo RAN, 2005. 356 p. (Rus)

14. Malyigin, G.A. (2007). *Fizika tverdogo tela* [Physics of solis], 49, 961. (Rus)

15. Koneva, N.A., Zhdanov, A.N. and Kozlov E.V. (2006*). Izvestiya RAN, Ser. fiz.*70, 577. (Rus)

16. Meyers, M.A., Mishra, A. and Benson, D.J. (2006). *Progr. Mater. Sci.*, 51, 472.

17. Tang. Z., and Sheng, P., ed. (2008). *Nanoscale Phenomena. Basic Science to Device Application*. N-Y.: Springer, 248 p.

18. Eletskiy, A.V. (2007). *Uspehi fiz. Nauk* [Advances in physical sciences], 177, 233. (Rus)

19. Schuh, C.A., Hufnagel, T.C. and Ramamurty, U. (2007). *Acta Mater*., 55, 4067.

20. Buecher, M.J.J. (2007). *Mater. Sci.*, 42, 8765.

21. Meyers, M.A., et al. (2008). *Progr. Mater. Sci.*, 53, 1.

22. Zhu, T., and Li, J. (2010). *Progr. Mater. Sci.*, 55, 710.

23. Gusev, A.I. (2005). *Nanomaterialyi, nanostrukturyi, nanotehnologii.* [Nanomaterials, nanostructures, nano-technologies], M.: Fizmatlit, 416 p. (Rus)

24. Bhushan, B., ed. (2008). *Nanotribology and Nanomechanics. An Introduction*. Berlin-Heidelberg: Springer-Verlag, 1516 p.

25. Golovin, Yu.I. (2007). *Vvedenie v nanotehniku* [Introduction to nanotechniques]. M.: Mashinostroenie, 496 p. (Rus).

26. Andrievskiy, R.A. and Ragulya, A.V. (2005). *Nanostrukturnyie materialyi* [Nanostructured materials]. M.: Akademiya, 192 p.

27. Meyers, M.A. and Chawla, K.K. (2009). *Mechanical Behavior of Materials*. Cambridge: CUP, 856 p.

28. Dao, M., et al. (2007). *Acta Mater*., 55, 4041.

29. Koch, C.C., et al. (2010). *J. Mater. Sci.*, 45, 4725.

30. Schmander, S. and Mishnaevsky, L. Jr. *Micromechanics and Nanosimulation of Metals and Composites. Advanced Methods and Theoretical Concepts.* Berlin, Heidelberg: Springer, 420 p.

31. Sharma, K.R. (2010). *Nanostructuring operations in Nanoscale Science and Engineering.* NY: Mc Graw-Hill, 292 p.

32. Cat, D.T., Pussi, A. and Wandelt, K., ed. (2009). *Physics and Engineering of New Materials*. Berlin-Heidelberg: Springer, 387 p.

33. Bansal, N.P. and Singh, J.P., ed. (2009). *Processing and Properties of Advanced Ceramics and Composits*. Hoboken, N.J.: Wiley, 256 p.

34. Chung, D.D.L. (2010). *Composite Materials. Science and Applications.* London: Springer, 349 p.

35. Koch C.C., et al. (2007). *Structural Nanocrystalline Materials. Fundamental and Applications.* Cambridge: Cambridge University Press, 364 p.

36. Gusev, E., Garfunkel, E. and Dideikin, A., ed. (2010). *Advanced Materials and Technologies for Micro/Nanodevices, Sensors and Actuators*. New York: Springer Science, 314 p.
37. Wilde, G., ed. (2009). *Nanostructured Materials* Amsterdam: Elsevier, 374 p.
38. Shakelford, J.F. and Doremus, R.H. (2008). *Ceramic and Glass Materials. Structure, Properties and Processing*. New York: Springer Science, 201 p.
39. Ohno, K., ed. (2008). *Nano- and Micromaterials*. Berlin, Heidelberg: Springer, 337 p.
40. Serdyuk, I., Zakkai, N. and Zakkai, Dzh. (2010). *Metodyi v molekulyarnoy biofizike* [Methods in molecular biophysics], V.2. M.: KDU, 739 p. (Rus)
41. Makmillan, N. (1987). *Atomistika razrusheniya* [Atomic theory of destruction]. M.: Mir.Pp. 35-103.
42. Ogata, S., et al. (2004). *Phys. Rev*., B70, 104104.
43. Zhu, T., et al. (2008). *Phys. Rev. Let*., 100, 025502.
44. Zhu, T., Li, J., Ogata, S. and Sidney, Y. (2009). *MRS Bull,* 34, 167.
45. Cheng, Y.Q. and Ma, E.(2011). *Acta Mater*., 59, 1800.
46. Golovin, Yu.I. (2009). *Perspektivnyie materialyi* [Prospective materials], V. 3. Tambov.: Izd-vo TGU-MISIS, P. 141. (Rus)
47. Koneva, N.A. and Kozlov, E.V. (2009). *Perspektivnyie materialyi* [Prospective materials], V. 3. Tambov: Izd-vo TGU-MISIS, P. 267.
48. Oliver, W.C. and Pharr (2004). G.M. *Mater. J. Res*. 19. 3.
49. ISO, 2007, 14557-4: 2007. Metallic Materials - Instrumented Indentation Test for Hardness and Materials Parameters – Part 4: Test Method for Metallic and Non-Metallic Coatings. ISO, Geneva, Switzerland.
50. ASTM, 2007, E 2546-07, Standard Practice for Instrumented Indentation Testing. ASTM International, West Conshohocken, PA, USA.
51. Burgess, T. and Ferry, M. (2009). *Materials Today*. 12, 24.
52. Golovin, Yu.I. (2009). *Nanoindentirovanie i ego vozmozhnosti* [Nanoindentation and its capabilities], M.: Mashinostroenie, 312 p. (Rus)
53. Golovin, Yu.I., Tyurin, A.I. and Hlebnikov V.V. (2000). ZhTF.70, 82.
54. Fischer-Cripps, A.C. (2002). *Nanoindentation*. New York: Springer, 198 p.
55. VanLandingham, M.R. (2003). *J. of Res. of NIST*., 4, 249.
56. Fischer-Cripps, A.C. (2006). *Surface Coating Technol.,* 14-15, 4153.
57. Schuh, C.A. (2006). *Materials Today*, 5, 32.
58. Gouldstone, A., et al. (2007). *Acta Mater.*, 55, 4015.
59. Chudoba, T. (2006). *Measurement of Hardness and Young's Modulus by nanoindentation. In: Nanostructured Coatings* (*eds*. Cavaleiro, A. and De Hosson, J.T.M.). New York: Springer, P. 216-260.
60. Herrmann, K. (2007). *Härteprüfung an Metallen und Kunststoffen*. Expert Verlag. Renningen, 258 p.
61. Lucca. D.A., Herrmann. K. and Klopfstein M.J. (2010). *CIRP Annals Manufactoring Technolog,*. 59, 803.
62. Golovin, Yu.I. (2008). *Physics of Solids,* 50, 2113.
63. Golovin, Yu.I. (2009). *Zavodskaya laboratoriya. Diagnostika materialov* [Plant Laboratory. Materials Diagnostics], 75, 37. (Rus).
64. Golovin, Yu.I. (2009). Zavodskaya laboratoriya. Diagnostika materialov [Plant Laboratory. Materials Diagnostics], 75, 45.
65. Stark, R.W. (2010). *Materials Today,* 13, 24.
66. Smith, R.L. and Mecholsky, J.J. Jr. (2011). *Materials Characterisation,* 62, 457.
67. Park, J.Y., et al. (2010). *Materials Today,* 13, 38.
68. *Noy, A.,* ed. (2008). *Handbook of Molecular Force Spectroscopy*. Berlin-Heidelberg: Springer, 300 p.
69. Greenleaf, W.J., Woodside, M.T. and Block S.M. (2007). *Annual Review of Biophysics and Biomolecular Structure,* 36, 171.
70. Neuman, K.C. and Nagy, A. (2008). *Nature Methods,* 5, 491.
71. Conroy, R. (2008). Force Spectroscopy with Optical and Magnetic Tweezers. In: Handbook of Molecular Force Spectroscopy (Noy, A., ed.). Springer, P. 23-96.
72. Beyer, M.K. and Clancen-Schaumann, H. (2005). *Chemical Rewiews,* 105, 292.
73. Lee, Ch.-K., et al. (2007). *Micron*, 38, 446.
74. Fisher-Cripps, A. C. (2009). *The IBIS Handbook of Nanoindentation.* Fisher-Cripps Laboratories, Australia, 259 p.
75. Yang, F. and Li, J.C.M., ed. (2008). *Micro and Nano Mechanical Testing of Materials and Devices*. New York: Springer, 387 p.
76. Pharr, G.M., Strader, J.H. and Oliver, W.C. (2009). *J. Mater. Res.*, 24, 653.
77. Dub, S.N., Lim, V.Y. and Chandhri, M.M. (2010). *J. Appl. Phys.,* 107, 043510.
78. Dehm, G. (2009). *Progress in Materials Sci.,* 54, 664.
79. Zhu, Y., Ke, C. and Espinosa H.D. (2007). *Experimental Mechanics*. 10, 256.
80. Demir, E., Raabe, D. and Roters F. (2010). *Acta Mater*., 58, 1876.
81. Lee, S.-W., Han, S.M. and Nix W.D. (2009). *Acta Mater*. 57, 4404.
82. Demir, E., et al.(2009). *Acta Mater*., 57, 559.
83. Lowry, M.B., et al. (2010). *Acta Mater*., 58, 5160.
84. Withey, E.A., et al. (2010). Acta Mater., 58, 2652.
85. Ye, J., et al. (2010). *Acta Mater*., 58, 490.
86. Zhang, L., et al. (2011). *Scripta Mater.,* 64, 919.
87. Hurley, D.S., Kopycinska-Müller, M. and Kos, A.B. (2007). *JOM*. 59, 23.
88. Caron, A., Arnold, W. (2009). *Acta Mater*., 57, 4353.
89. Bhushan, B. and Fuchs, H., ed. (2009). *Applied Scanning Probe Methods XI*. Berlin-Heidelberg: Springer-Verlag, 2009. 235 p.
90. Lee, G., et al. (2010). *Acta Mater*., 58, 1361.
91. Deluca, M., et al. (2010). *Scripta Mater*., 63, 343.
92. Golovin, Yu., Tyurin, A. and Farber, B. (2002). *J. Mater. Sci*., 37, 895.
93. Ruffel, S., Bradby, J.E. and Williams, J.S. (2007). *J. Mater. Res*., 22, 578.
94. Parket, J.Y., et al. (2010). *Materials Today*, 13, 38.
95. Giridharagopal, R., et al. (2010). *Materials Today*, 13, 50.
96. Ebenstien, Y., et al. (2009). *J. of Molecular Recognition*, 1, 6.
97. Jarvie, H.P. and King, S.M. (2010). *Nano Today*, 5, 248.
98. Mulholland, M.D. and Seidman, D.N. (2011). *Acta Mater.*, 59, 1881.

XX
MENDELEEV CONFERENCE
ON GENERAL AND APPLIED CHEMISTRY

September 26-30, 2016
Ekaterinburg, Russia

Conference Schedule

Plenary meetings, sessions, poster presentations, and round-table discussions on the main directions of chemical science and technology, and chemical education are included in the programme of XX Mendeleev Conference.

Sessions

1. **Fundamental Problems of Chemical Science**
Moderators: O.M. Nefedov (Academician of RAS) M.P. Egorov (Academician of RAS), O.N. Chupakhin (Academician of RAS)

2. **Chemistry and Technology of Materials and Nanomaterials**
Moderators: E.N. Kablov (Academician of RAS), N.T. Kuznetsova (Academician of RAS), V.V. Ustinov (Academician of RAS)

3. **Physical and Chemical Fundamentals of Metallurgical Processes**
Moderators: L.I. Leontiev (Academician of RAS), O.A. Bannykh (Academician of RAS), K.A. Solntsev (Academician of RAS), L.A. Smirnov (Academician of RAS)

4. **Problems of Chemical Industry, Technical Risks Assessment**
Moderators: Professor S.V. Golubkov, A.E. Gerdt

5. **Chemical Aspects of Modern Power Engineering and Alternative Energy Resources**
Moderators: A.Yu. Tsivadze (Academician of RAS), I.I. Moiseev (Academician of RAS), Professor Yu.P. Zaikov

6. **Chemistry of Fossil And Renewable Hydrocarbon Raw Materials**
Moderators: V.N. Parmon (Academician of RAS), S.N. Khadzhiev (Academician of RAS), V.S. Zagainov

7. **Analytical Chemistry: New Methods and Devices for Chemical Research and Analysis**
Moderators: Yu.A. Zolotov (Academician of RAS), Professor A.I. Matern

8. **Medical Chemistry: Fundamental And Applied Aspects**
Moderators: N.S. Zefirov (Academician of RAS), V. N. Charushin (Academician of RAS), A.P. Petrov

9. **Chemical Education**
Moderators: V .V. Lunin (Academician of RAS), O.I. Koifman (Corresponding Member of RAS) V.L. Rusinov (Corresponding Member of RAS)

Registration and Abstract Submission

Please submit your application and abstract up to one page in Russian and English using the form at the website www.mendeleev2016.uran.ru.

Contact Information

Organizing Committee of XX Mendeleev Conference (Scientific Secretaries):
Doctor of Chemical Science, Professor Yulia Germanovna Gorbunova,
Frumkin Institute of Physical Chemistry and Electrochemistry RAS
119991 Moscow, Russia, 31, Bulding 4 Leninsky Prospect,
Phone number: +7 495 955 48 74
E-mail: mendeleev2016@gmail.com

PD in Chemical Sciences Olga Aleksandrovna Kuznetsova,
Ural Branch of Russian Academy of Science
620990 Ekaterinburg, Russia, Pervomayskaya 91,
Phone number: +7 343 374 34 77
E-mail: mendeleev@prm.uran.ru